TABLE I
SUMMARY OF THERMAL, MECHANICAL, AND MICROWAVE PROPERTIES OF SUPERCONDUCTING COAXIAL RIBBON CABLE, LAMINATED MICROSTRIP CABLE, AND BEST COMMERCIALLY AVAILABLE SUPERCONDUCTING COAXIAL CABLES

Cable	**Thermal Load**[8] per trace [nW] 100mK to 1 K	4 K	**Mechanical** All Dimensions [mm] Trace Pitch	OD (∅)	Min. Inside Bend Radius	Conductor Material	Dielectric Material	**Microwave** Values at 8GHz Cross Talk [dB]	Attenuation[9] [dB]
FLAX	16	800	3.556	0.376	2	Nb47Ti	PFA	−60	1
CryoCoax	26	1400	>13	0.900	3.2	NbTi	PTFE	N/A	< 0.5
KEYCOM	34	1800	>13	0.860	8	NbTi	PTFE	N/A	< 0.5
Nikaflex	16	460	3.556	0.198[10]	6.4	Nb47Ti	Nikaflex[11]	−25	1

[8] Computed using dimensions available from [15], [20], [21] and assuming a cable length of 30 cm.
[9] Estimated with ripple peak.
[10] For the microstrip geometry this is the total cable thickness.
[11] Kapton polyimide film manufactured by Dupont, see [15] for details.

what we previously achieved using flexible laminated NbTi-on-Kapton microstrip cables [15]. Since the cable's installation in the MKID Exoplanet Camera (MEC) at Subaru Observatory, this enhanced isolation has increased our pixel yield ∼20% [17]. We suspect this large improvement is because the exposed microstrip geometry allows trace-to-trace coupling, whereas the coaxial nature of the FLAX shields the center conductors thereby preventing signal corruption. In early iterations of the cable, we found infrequent or failed microspot welds in the ground shield lead to much higher levels of cross talk. This leads us to conclude incorporating microspot welds less than $\lambda/16$ apart between the traces reduces electromagnetic coupling.

C. Thermal Conductivity

Following previous convention, a cable thermal conductivity, $G(T)$, was computed by summing literature values of constituent materials weighted by their cross-sections (see Fig. 6) [15], [23]. We compare our superconducting coaxial ribbon cable to two commercially available superconducting coaxial cables as well as our lab's previously developed laminated NbTi-on-Kapton microstrip cables [15]. We estimate the thermal conductivity of the PFA dielectric present in the flexible coaxial ribbon cables using PTFE; the same dielectric used in the two commercial solutions [22]. The smallest commercially available superconducting coaxial cables from KEYCOM[12] and CryoCoax[13] were chosen for comparison. The electrical and thermal properties of the cables are summarized in Table I.

The heat load from one temperature stage to another can be computed by integrating values in Fig. 6 from T_1 to T_2 ($T_1 < T_2$) and dividing by the cable length. The ten-trace FLAX cables are currently installed in the MEC experiment where they span 33 cm from the 3.4 K stage to the 90 mK cold ADR stage with a thermal sink at 800 mK about halfway down the length of the cable [18]. We estimate they generate a thermal load of ∼200 nW on the 90 mK cold ADR stage. This is about equivalent to the thermal load created by the Nikaflex cables and approximately half the computed heat load of either commercial option.

[12] KEYCOM Corp. 3-40-2 Minamiotsuka,Toshima-ku Tokyo. P/N: NbTiNbTi034
[13] CryoCoax - Intelliconnect, 448 Old Lantana Road, Crossville, TN. P/N: 5139-P1NN-611-100P

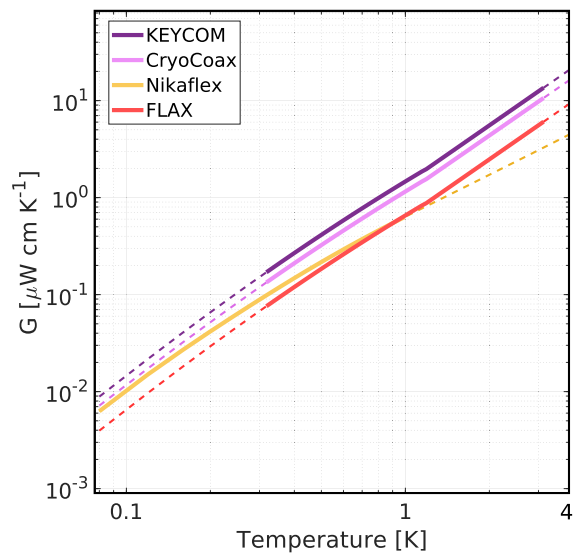

Fig. 6. We computed a cable thermal conductivity $G(T)$ in units of $\mu\mathrm{WcmK}^{-1}$ by summing the thermal conductivity of each constituent material weighted by the cross-section [15], [23]. The cable previously developed by our lab (Nikaflex, gold) is compared with the subject of this article (FLAX, salmon), and two commercial options by KEYCOM (P/N: NbTiNbTi034, burgundy) and Cryocoax (P/N 5139-P1NN-611-100P, pink). Solid lines are computed using literature values for Nb47Ti [24], [25], PTFE [23], Nikaflex (Kapton polyimid film) [15], [26], and Pyralux [24]. PTFE values were used to estimate the PFA dielectric in the FLAX cable [22]. Dashed lines indicate extrapolation.

IV. CONCLUSION

We have manufactured a superconducting flexible coaxial cable capable of delivering microwave signals between temperature stages with minimal loss, cross talk, and heat conduction. Strong signal isolation is especially important for our application of moving 4–8 GHz servicing 10 000+ multiplexed sensors across temperature stages. The FLAX cable represents a 30 dB improvement in cross talk as compared to our group's previously developed NbTi-on-Kapton microstrip cables. This enhanced isolation facilitated a ∼20% increase in MKID pixel yield in the MEC experiment [17]. We expect these results will be especially useful for high-density microwave superconducting detector arrays requiring strong signal isolation.

The cable technology presented in this article also has very low thermal conductivity. For a given thermal budget, the FLAX

Authorized licensed use limited to: UNIV OF ALABAMA-TUSCALOOSA. Downloaded on June 02,2023 at 20:22:13 UTC from IEEE Xplore. Restrictions apply.

cables allow for twice as many detectors as the leading commercial option. The reduced heat load combined with the push-on, small form factor connectors and reduced trace pitch allow for increased detector density in a cryogenic system.

We found an attenuation of 1 dB at 8 GHz with ∼3 dB ripples which is at worst 2× more loss than commercial options. This magnitude of ripples and loss do not impact our array on the input side as we can drive microwave resonators (MKIDs) located at transmission dips with higher power than their frequency neighbors. However, these features degrade the overall signal to noise ratio on the output. Ripples and loss may become prohibitive for systems operating at frequencies over 8 GHz or systems constrained by amplifier dynamic range. Insertion loss and ripples can be reduced by improving manufacturing precision in the forming of the NbTi foil crimps and location of microspot welds. Alternative methods to join the push on connectors and traces, e.g., brush plating the NbTi center conductor with an easily solderable material such as nickel may also improve the impedance match.

Finally, we note these cables are relatively easy to fabricate. Many components, most notably the fine, NbTi center conductor wire, are commercially available. All cable iterations were manufactured in-house at the University of California, Santa Barbara. Ten trace FLAX can be assembled in two days. Overall, we find this cable technology to be superior to commercial options for our applications building high-density superconducting detector arrays.

References

[1] R. Barends *et al.*, "Superconducting quantum circuits at the surface code threshold for fault tolerance," *Nature*, vol. 508, no. 7497, pp. 500–503, 2014.

[2] R. Barends *et al.*, "Digitized adiabatic quantum computing with a superconducting circuit," *Nature*, vol. 534, no. 7606, pp. 222–226, 2016. [Online]. Available: http://dx.doi.org/10.1038/nature17658

[3] N. Ofek *et al.*, "Extending the lifetime of a quantum bit with error correction in superconducting circuits," *Nature*, vol. 536, no. 7617, pp. 441–445, Jul. 2016. [Online]. Available: https://www.nature.com/articles/nature18949

[4] X. Gu, A. F. Kockum, A. Miranowicz, Y. x. Liu, and F. Nori, "Microwave photonics with superconducting quantum circuits," *Phys. Rep.* vol. 718–719, Nov. 2017, pp. 1–102.

[5] E. E. Wollman *et al.*, "Kilopixel array of superconducting nanowire single-photon detectors," *Opt. Express*, vol. 27, no. 24, Nov. 2019, Art. no. 35279.

[6] G. Ulbricht, B. A. Mazin, P. Szypryt, A. B. Walter, C. Bockstiegel, and B. Bumble, "Highly multiplexible thermal kinetic inductance detectors for X-ray imaging spectroscopy," *Appl. Phys. Lett.*, vol. 106, no. 25, Jun. 2015, Art. no. 251103. [Online]. Available: http://aip.scitation.org/doi/10.1063/1.4923096

[7] W. S. Holland *et al.*, "SCUBA-2: The 10 000 pixel bolometer camera on the James Clerk Maxwell telescope," *Monthly Notices Roy. Astronomical Soc.*, vol. 430, no. 4, pp. 2513–2533, 2013.

[8] M. Calvo *et al.*, "The NIKA2 instrument, a dual-band kilopixel KID array for millimetric astronomy," *J. Low Temp. Phys.*, vol. 184, no. 3/4, pp. 816–823, Aug. 2016.

[9] B. A. Mazin *et al.*, "ARCONS: A 2024 pixel optical through near-IR cryogenic imaging spectrophotometer," *Publications Astronomical Soc. Pacific*, vol. 125, no. 933, pp. 1348–1361, Nov. 2013.

[10] S. R. Meeker *et al.*, "Design and development status of MKID integral field spectrographs for high contrast imaging," in *Proc. Adaptive Opt. Extremely Large Telescopes 4—Conf. Proc.*, 2015, pp. 4–8.

[11] S. R. Meeker *et al.*, "DARKNESS: A microwave kinetic inductance detector integral field spectrograph for high-contrast astronomy," 2018. [Online]. Available: https://doi.org/10.1088/1538-3873/aab5e7

[12] C. G. Pappas *et al.*, "High-density superconducting cables for advanced ACTPol," *J. Low Temp. Phys.*, vol. 184, no. 1/2, pp. 473–479, Jul. 2016.

[13] D. B. Tuckerman *et al.*, "Flexible superconducting Nb transmission lines on thin film polyimide for quantum computing applications," *Supercond. Sci. Technol.*, vol. 29, no. 8, Jul. 2016, Art. no. 084007. [Online]. Available: https://iopscience.iop.org/article/10.1088/0953-2048/29/8/084007/meta

[14] S. Zou *et al.* , "Low-loss cable-to-cable parallel connection method for thin-film superconducting flexible microwave transmission lines," *Supercond. Sci. Technol.*, vol. 32, no. 7, May 2019, Art. no. 075006. [Online]. Available: https://iopscience.iop.org/article/10.1088/1361-6668/ab1825/meta

[15] A. B. Walter, C. Bockstiegel, B. A. Mazin, and M. Daal, "Laminated NbTi-on-Kapton microstrip cables for flexible sub-kelvin RF electronics," *IEEE Trans. Appl. Supercond.*, vol. 28, no. 1, pp. 1–5, 2018.

[16] V. Gupta *et al.*, "Thin-film Nb/Polyimide superconducting stripline flexible cables," *IEEE Trans. Appl. Supercond.*, vol. 29, no. 5, pp. 1–5, Aug. 2019.

[17] A. B. Walter *et al.*, "The MKID exoplanet camera for Subaru SCExAO," to be published.

[18] A. B. Walter, "MEC: The MKID exoplanet camera for high speed focal plane control at the subaru telescope," Ph.D. dissertation, Dept. Phys. Astron., Univ. California, Santa Barbara, USA, 2019.

[19] F. Gisin, "Characterizing lossy PCB interconnects using a TDR instrument," Multek, New Territories, Hong Kong, Tech. Rep., Mar. 2017. [Online]. Available: https://www.multek.com/sites/default/files/2017-09/TDR Measurements of PCB Interconnect Artifacts.pdf

[20] CryoCoax, "Cryogenic cable and cable assemblies | CryoCoax." [Online]. Available: https://cryocoax.com/cryogenic-cable-and-cable-assemblies/, Accessed on: Jun. 5, 2020.

[21] KEYCOM, "Superconducting coaxial cable assemblies (0.085" type NbTi-NbTi superconducting coaxial cables)." [Online]. Available: https://keycom.co.jp/eproducts/upj/Superconducting coaxial cable assemblies2/page.htm, Accessed on: Jun. 5, 2020.

[22] Emerson, "PTFE and PFA similarities and differences," Emerson Automation Solutions, Shakopee, Tech. Rep., 2017. [Online]. Available: https://www.emerson.com/documents/automation/white-paper-ptfe-pfa-simil arities-differences-rosemount-en-585104.pdf

[23] A. Kushino, M. Ohkubo, and K. Fujioka, "Thermal conduction measurement of miniature coaxial cables between 0.3 and 4.5 K for the wiring of superconducting detectors," *Cryogenics*, vol. 45, no. 9, pp. 637–640, 2005.

[24] M. Daal, N. Zobrist, N. Kellaris, B. Sadoulet, and M. Robertson, "Properties of selected structural and flat flexible cabling materials for low temperature applications," *Cryogenics*, vol. 98, pp. 47–59, Mar. 2019.

[25] J. R. Olson, "Thermal conductivity of some common cryostat materials between 0.05 and 2 K," *Cryogenics*, vol. 33, no. 7, pp. 729–731, 1993.

[26] N. Kellaris *et al.*, "Sub-kelvin thermal conductivity and radioactivity of some useful materials in low background cryogenic experiments," *J. Low Temp. Phys.*, vol. 176, no. 3/4, pp. 201–208, Jan. 2014.

Authorized licensed use limited to: UNIV OF ALABAMA-TUSCALOOSA. Downloaded on June 02,2023 at 20:22:13 UTC from IEEE Xplore. Restrictions apply.